Ruthenium Tetraammines as a Model of Nitric Oxide Donor Compounds

José Carlos Toledo,[a] Hildo A. S. Silva,[a] Marciela Scarpellini,[a] Vânia Mori,[b] Ademir J. Camargo,[a] Mauro Bertotti,[b] and Douglas W. Franco*[a]

Dedicated to our friend and colleague Luiz Manoel Aleixo in memoriam

Keywords: Nitric oxide / Ruthenium / NO donor / N-heterocyclic ligands

The nitric oxide liberation from *trans*-$[Ru(NH_3)_4(L)(NO)]^{3+}$ (where L = py, 4-pic, isn, nic, L-His, 4-Clpy, imN) after one-electron-chemical or electrochemical reduction was investigated through spectroscopic and electrochemical techniques, reaction-product analysis and quantum-mechanic calculations. These complexes can be formally viewed as a $Ru^{II}(NO^+)$ species and the reduction site is located on the NO ligand. The $E°$ for the *trans*-$[Ru^{II}(NH_3)_4(L)(NO^+)]^{3+}$/*trans*-$[Ru^{II}(NH_3)_4(L)(NO)]^{2+}$ redox process ranges from 0.072 V vs. NHE (nic) to –0.118 V vs. NHE (imN). The specific rate constants for NO dissociation from *trans*-$[Ru^{II}(NH_3)_4(L)(NO)]^{2+}$, evaluated through double-step chronoamperometry, range from 0.025 s^{-1} (nic) to 0.160 s^{-1} (ImN) at 25 °C. The $[Ru^{II}NO^+/Ru^{II}NO^0]$ redox potential and the specific rate constant (k_{-NO}), key steps for designing nitrosyl complexes as NO-donor drug prototypes, proved to be controlled by a judicious choice of the ligand (L) trans to NO.

Introduction

Since the physiological roles of nitric oxide (NO) were discovered,[1,2] a great deal of effort has been put into the development of NO-carrier drugs.[3,4] The great affinity of d^6 and d^5 low-spin-metal complexes for NO and the versatility of NO on its own right as a ligand[5–7] make the nitrosyl complexes a good alternative for such a proposal.[8,9] Indeed, many metal complexes have been suggested as both promising NO scavengers and NO donors.[10–17] In general, the bonding between a d^6 low-spin-metal center and NO, which preferably assumes the MNO^+ form, is remarkably strong.[5,6] Therefore, for tailoring NO-donor compounds, procedures to generate MNO^0 species, in which NO is labile, are essential. Strategies involving photochemistry[18,19] and reduction activation[20] of nitrosyl complexes have been proposed as alternatives.

In this context, the photochemical[9,21,22] and reductive pathways[9,15,16] to induce NO liberation in *trans*-$[Ru(NH_3)_4(L)(NO)]^{3+}$ complex ions have been explored. This is a promising system, since these complexes are generally resistant to air oxidation and are water-soluble and robust under physiological conditions.[21,22] Furthermore, it is well-known that ammine ligands localized in the equatorial positions are inert towards substitution reactions,[23] allowing the control of the NO reactivity in relation to the properties of the ligand trans to NO. This paper reports on the activation of the *trans*-$[Ru(NH_3)_4L(NO)]^{3+}$ species, (where L = N-heterocyclic ligands) to induce NO release through reduction. Two main requirements for these complexes to work as NO donors in biological media are: i) the reduction potential of coordinated NO must be accessible to biological reducing agents; ii) it is necessary to control the dissociation of NO^0 from the intermediate *trans*-$[Ru(NH_3)_4L(NO)]^{2+}$. As described here, both requirements can be fulfilled by means of a judicious choice of L.

Results and Discussion

The systems dealt with in this study, the *trans*-$[Ru(NH_3)_4(L)(NO)]^{3+}$ complex ions, are EPR silent. In addition, their ν_{NO} is always higher than 1900 cm^{-1} and the Ru–N–O angle obtained by X-ray crystallography is close to 180°: *trans*-$[Ru(NH_3)_4(nic)(NO)](SiF_6)_3$ (177.0°),[21] *trans*-$[Ru(NH_3)_4(H_2O)(NO)]Cl_3$ (178.1°),[24] *trans*-$[Ru(NH_3)_4(4\text{-pic})(NO)](SiF_6)(BF_4)\cdot H_2O$ (178.6°) and *trans*-$[Ru(NH_3)_4P(OEt)_3(NO)](CF_3COO)_3$ (174.9°).[25] Based on these properties, it is reasonable to assign the $[Ru^{II}NO^+]$ formula to all these *trans*-$[Ru(NH_3)_4(L)(NO)]^{3+}$ complexes. The result of the reaction with hydroxide ions, always yielding the corresponding nitro compound,[9,21,22,26] *trans*-$[Ru(NH_3)_4(L)(NO_2)]^+$, confirms the nitrosonium character of the NO ligand in such species.

[a] Instituto de Química de São Carlos, Universidade de São Paulo, Av. Trabalhador SãoCarlense 400, 13560-970 São Carlos, Brazil
Fax: (internat.) +55-16-2739976
E-mail: douglas@iqsc.usp.br
[b] Instituto de Química, Universidade de São Paulo, Av. Prof. Lineu Prestes 748, 05508900 São Paulo, Brazil

It is well-known that nitrosyl complexes in aqueous solution react with hydroxide ions yielding the respective nitro compounds (see Equation 1), depending on both the pH of the solution and the nature of L.[5,6,21,22,26] Since nitro compounds are not expected to exhibit the hypotensive effect observed in nitrosyl complexes, the equilibrium established between the two species, *trans*-$[Ru(NH_3)_4L(NO)]^{3+}$ and *trans*-$[Ru(NH_3)_4L(NO_2)]^{+}$, in physiological pH, is a fundamental factor to be considered when utilizing nitrosyl complexes as nitric oxide donors. According to the K_{eq} data[9,21,22,26] for Equation 1, the *trans*-$[Ru(NH_3)_4L(NO)]^{3+}$ form accounts for more than 98 % of the nitrosyl complexes at pH 7.

$$trans\text{-}[Ru(NH_3)_4L(NO)]^{3+} + 2\,OH^- \overset{K_{eq}}{\rightleftharpoons} trans\text{-}[Ru(NH_3)_4L(NO_2)]^{+} + H_2O \quad (1)$$

Cyclic voltammograms of *trans*-$[Ru(NH_3)_4(L)(NO)]^{3+}$ aqueous solutions show only one monoelectronic redox process between −0.6 V and 1.0 V versus SCE,[21,22] which was attributed to the couple $Ru^{II}NO^+/Ru^{II}NO^0$, in Equation (2):

$$trans\text{-}[Ru^{II}(NH_3)_4(L)(NO^+)]^{3+} + e^- \longrightarrow trans\text{-}[Ru^{II}(NH_3)_4(L)(NO^0)]^{2+} \quad (2)$$

DFT computation[27] for *trans*-$[Ru^{II}(NH_3)_4(L)(NO^+)]^{3+/2+}$ (where L = NH_3, Cl^-, OH^-, py and pz), indicates that the LUMO is always predominantly on the π* of NO (68−70%), although the HOMO is dependent on the nature of L: 90−95 % Ru (dxy) for L = NH_3, Cl^-, OH^- and 100 % L (πL) for L = pyridine and pyrazine. Thus, the one-electron reduction of these complexes is expected to generate $[Ru^{II}NO^0]$ species. Indeed, the coordinated NO radical have been detected through electron paramagnetic-resonance spectroscopy[28] for the reduced form of the *trans*-$[Ru(NH_3)_4(H_2O)(NO)]^{3+}$ ion. Considering the structural and chemical similarities among all title complexes, such behavior is expected to be general for the whole series. A similar EPR spectrum[28] was also observed for the one-electron reduced species of *trans*-$[RuPP(Cl)(NO)]^{2+}$ PP = $(C_2H_5)_2P(CH_2)_2P(C_2H_5)_2$ or $(C_6H_5)_2P(CH_2)_2P(C_6H_5)_2$, *trans*-$[Ru(cyclam)(Cl)(NO)]^{2+}$ and $[Ru(bipy)_2(Cl)(NO)]^{2+}$.[29]

The reduced species, *trans*-$[Ru(NH_3)_4(L)(NO)]^{2+}$, releases NO^0 according to Equation (3).

$$trans\text{-}[Ru(NH_3)_4(L)(NO)]^{2+} + H_2O \longrightarrow trans\text{-}[Ru(NH_3)_4(L)(H_2O)]^{2+} + NO^0 \quad (3)$$

The presence of free NO in solution, after reduction of the nitrosyl complexes, was detected by cyclic voltammetric and differential-pulse polarographic experiments ($E°$ NO^+/NO^0 = +0.80 V vs. SCE).[30−32] The presence of the resulting aqua species, *trans*-$[Ru(NH_3)_4(L)(H_2O)]^{2+}$, was also evident from the electronic spectra and voltammetric behavior. Furthermore, the resulting solutions are EPR silent at liquid nitrogen temperature.

The *trans*-$[Ru(NH_3)_4L(NO)]^{2+}$ ions were generated through chemical [Cd(Hg) and Eu^{II}] or electrochemical reduction. Figure 1 shows typical UV/Vis spectra for *trans*-$[Ru(NH_3)_4(py)(NO)]^{3+}$, when the solution is electrolyzed in a spectroelectrochemical experiment as a function of time. The observed bathochromic shift (from λ_{226} and λ_{267} to λ_{256} and λ_{330})[33] is consistent with the lower π-acceptor ability of the NO^0 ligand relative to the NO^+ ligand. The appearance of a band at 406 nm during the experiment is in agreement with the formation of *trans*-$[Ru(NH_3)_4(py)(H_2O)]^{2+}$, since this species absorbs strongly in this region (ε_{406} = 3.4 × 10^3 M^{-1} cm^{-1}).[32]

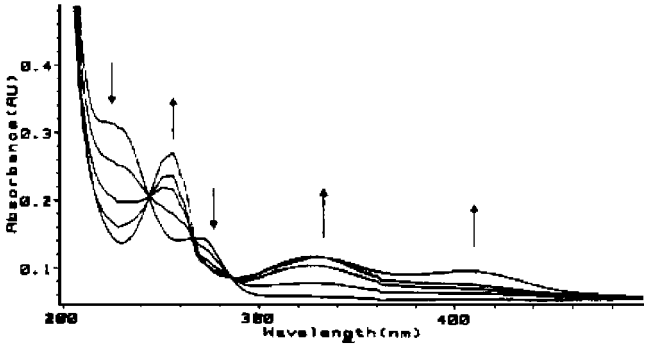

Figure 1. UV/Vis spectra for solutions containing *trans*-$[Ru(NH_3)_4(py)(NO)]^{2+}$ ions subjected to electrolysis as a function of time (applied potential: −0.40 V vs. SCE; μ = 0.1 $NaCF_3COO$; T = 15 °C, [Ru] = 5.0 × 10^{-4} M)

As expected, the chemical reduction of the *trans*-$[Ru(NH_3)_4L(NO)]^{3+}$ ions using Eu^{II} ions or Cd(Hg) also produces the respective aqua species. Differential-pulse polarographic experiments of *trans*-$[Ru(NH_3)_4(py)(NO)]^{3+}$ solutions show that after the addition of Eu^{II} ions ($E°$ = −0.60 V vs. SCE), the reduction wave corresponding to the $Ru^{II}NO^+/Ru^{II}NO^0$ redox process completely disappears with the simultaneous formation of a redox wave, which corresponds to the Ru^{III}/Ru^{II} couple in *trans*-$[Ru(NH_3)_4(py)(H_2O)]^{2+}$. In addition, the IR spectrum of the resulting solution does not show the easily identifiable NO-stretching frequency at 1931 cm^{-1}, indicating that the NO ligand is no longer present in the ruthenium-coordination sphere.

The rate-constant values for NO dissociation were determined by double-potential-step chronoamperometry (see Table 1) and are consistent with the rate law:

d/dt [*trans*-$[Ru(NH_3)_4(L)(H_2O)]^{2+}$] = k_{-NO} [*trans*-$[Ru(NH_3)_4(L)(NO)]^{2+}$]

According to the data shown in Table 1, the rate constants for NO dissociation in *trans*-$[Ru(NH_3)_4(L)(NO)]^{2+}$ ions vary from 0.025 s^{-1} (isn) to 4.00 s^{-1} (imC) at 25 °C. The sequence of k_{-NO} as a function of L increases as follows: pic ≈ nic ≈ H_2O ≈ py < L-His ≈ imN < pz < imC, which is the same sequence observed for water[34] or

Table 1. Specific rate constants for NO^0 dissociation from *trans*-$[Ru(NH_3)_4(L)(NO)]^{2+}$, $[Ru^{II}NO^+/Ru^{II}NO^0]$ redox potential and electrochemical ligand parameters

Ion complex	[a] k_{-NO} (s^{-1})	$E^{0'}_{(NO+/NO)}$ (V vs. NHE)	ΣE_L
[b] *trans*-$[Ru(NH_3)_4(nic)(NO)]^{2+}$	0.025	0.072[21]	0.56
[b] *trans*-$[Ru(NH_3)_4(isn)(NO)]^{2+}$	0.043	0.052[21]	0.54
[b] *trans*-$[Ru(NH_3)_4(4\text{-pic})(NO)]^{2+}$	0.070	−0.008	0.51
[b] *trans*-$[Ru(NH_3)_4(4\text{-Clpy})(NO)]^{2+}$	0.030	0.012	0.54
[c] *trans*-$[Ru(NH_3)_4(H_2O)(NO)]^{2+}$	0.040[24]	−0.148[24]	0.32
[b] *trans*-$[Ru(NH_3)_4(py)(NO)]^{2+}$	0.060	0.012[21]	0.53
[b] *trans*-$[Ru(NH_3)_4(\text{L-His})(NO)]^{2+}$	0.140	−0.108[22]	0.42
[b] *trans*-$[Ru(NH_3)_4(imN)(NO)]^{2+}$	0.160	−0.118[22]	0.40
[b] *trans*-$[Ru(NH_3)_4(pz)(NO)]^{2+}$	0.070	0.112[21]	0.61
[c] *trans*-$[Ru(NH_3)_4(imC)(NO)]^{2+}$	4.000[20]	−0.298[20]	–
[c] *trans*-$[Ru(NH_3)_4P(OEt)_3(NO)]^{2+}$	0.980[25]	0.142[25]	0.68

[a] ($\mu = 0.1$, $NaCF_3COO$; $T = 25$ °C; [Ru] = 1.0×10^{-3} M, pH = 5). [b] Estimated by chronoamperometric method; most of the reported values are the average of at least three determinations; uncertainty of ± 15%. [c] Estimated by cyclic voltammetric method (Nicholson and Shain).

sulfate[32] lability in *trans*-$[Ru(NH_3)_4L(Y)]^{2+}$ complexes (where L = N-heterocyclic ligand, Y = H_2O or SO_4^{2-}).

According to the dissociative pathway for octahedral complexes, NO labilization should reflect the affinity of the *trans*-$[Ru(NH_3)_4(L)(H_2O)]^{2+}$ complex ions for the NO ligand and should be directly connected to the effective ruthenium charge in these complexes. Due to the similarities of the ion complexes studied, the ruthenium effective charge could be discussed on the basis of the electronic properties of the trans N-heterocyclic ligands. It is well-accepted that the higher the π-withdrawing ability of L, the more positive the redox potential of the $Ru^{III/II}$ couple and, therefore, the lower the specific rate constant for the dissociation of the ligand leaving. Since the $M^{n+/(n-1)+}$ redox potential is an indication of the metal-center-effective charge, it is expected that the higher the *trans*-$[Ru(NH_3)_4(L)(H_2O)]^{3+/2+}$ redox potential,[35] the lower the k_{-NO} value. Indeed, as observed for other leaving ligands, a linear tendency ($k_{-NO}/s^{-1} = -0.7 \times E^\circ$ *trans*-$[Ru(NH_3)_4(L)(H_2O)]^{3+/2+} + 0.07$; $R = 0.97$; pyrazine value not considered) is observed when the *trans*-$[Ru(NH_3)_4(L)(H_2O)]^{3+/2+}$ redox potential is plotted against the k_{-NO} values (see Figure 2). The ligand electrochemical parameter (E_L), introduced by Lever,[36] is known to be helpful in predicting the metal redox potential and we expected to find a correlation between the k_{-NO} values and the sum of E_L (ΣE_L) (see Table 1). This correlation exists and as can be observed in Figure 3 ($k_{-NO}/s^{-1} = -0.81 \times \Sigma E_L + 0.48$; $R = 0.997$, pyrazine value not considered). Since E_L values for a large number of N-heterocyclic ligands are available in the literature,[36] this correlation could become a very convenient tool for estimating the rate constants for NO dissociation from *trans*-$[Ru(NH_3)_4(L)(NO)]^{2+}$ species.

As observed in Table 1, the values for NO dissociation when L = pz, imC and $P(OEt)_3$ do not follow the trend observed for the other N-heterocyclic ligands (see Figure 3). The imC and $P(OEt)_3$ properties differ substantially from the N-based ligands as they are coordinated through carbon and phosphorus atoms, respectively. The trans labilizing effect of these two ligands is notable and therefore their

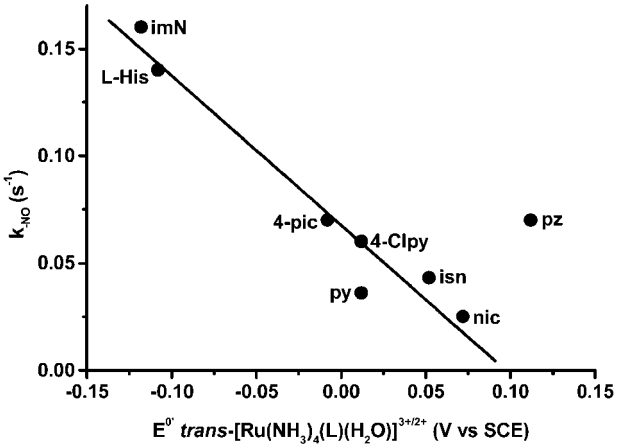

Figure 2. Correlation between the k_{-NO} values and $E^{\circ'}$ *trans*-$[Ru(NH_3)_4(L)(H_2O)]^{3+/2+}$ (V vs. SCE)

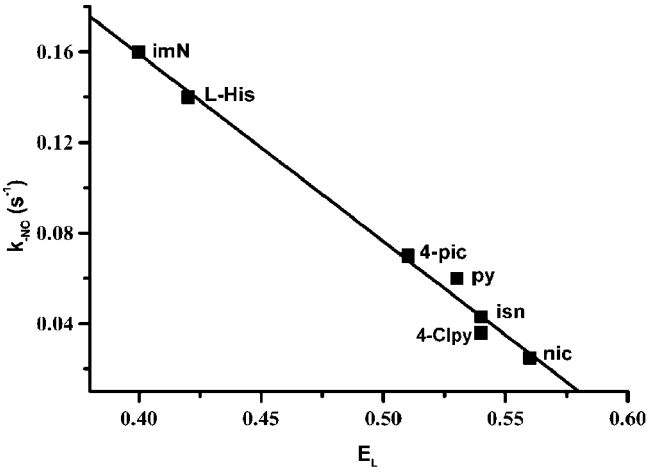

Figure 3. Correlation between the k_{-NO} values and ΣE_L ($\Sigma E_L = 4 \times E_L$ NH_3 + E_L L)

complexes do not fit the correlation implied by Figure 3 [imC and $P(OEt)_3$ values were omitted for clarity]. The behavior of the pyrazine ligand has not yet been understood

and is currently under investigation in our laboratory. However, the same behavior has been observed for pyrazine derivatives in studies on sulfate dissociation from *trans*-$[Ru(NH_3)_4(L)(SO_4)]$ (L = N-heterocyclic ligands).[32]

From the discussion above, it is clear that the $[Ru^{II}NO^+/Ru^{II}NO^0]$ reduction potential is one of the key steps in activating nitrosyl complexes to release NO. If the target is to tailor a compound that can be activated in vivo through reduction, the $[Ru^{II}NO^+/Ru^{II}NO^0]$ redox potential must be in a range suitable to reducing agents present in the biological medium. The $[Ru^{II}NO^+/Ru^{II}NO^0]$ redox potential for the nitrosyl complexes dealt with here (Table 1) ranges from −0.118 for L = imN to 0.072 V vs. NHE for L = nic, suggesting that all these complexes could be reduced by biological reducing agents[37] such as NADH, the flavin coenzymes $FADH_2$ and $FMNH_2$ and iron sulfur proteins. Recent studies have suggested that the *trans*-$[Ru(NH_3)_4P(OC_2H_5)_3(NO)]^{3+}$ nitrosyl complex can be reduced by mitochondrial reducing power[38] and that this compound exhibits an effective hypotensive effect in mice.[15,16] This biological activity is attributed to its NO-donor ability. The $[Ru^{II}NO^+/Ru^{II}NO^0]$ redox potential for *trans*-$[Ru(NH_3)_4L(NO)]^{3+}$ complexes was shown to be sensitive to the nature of the ligand L, trans to NO. This was expected, since the most accessible site for reduction in these complexes is localized on the nitrosyl ligand. Thus, the NO electronic density and therefore the $[Ru^{II}NO^+/Ru^{II}NO^0]$ redox potential are a function of the competition between the axial ligands, NO and L, on the ruthenium 4dπ electron density. Indeed, a correlation between the *trans*-$[Ru(NH_3)_4L(NO)]^{3+/2+}$ and the respective aqua species *trans*-$[Ru(NH_3)_4L(H_2O)]^{3+/2+}$ redox potential was observed. In addition, a linear correlation was also observed plotting the *trans*-$[Ru(NH_3)_4L(NO)]^{3+/2+}$ redox potential and the ligand electrochemical parameters ΣE_L (Table 1) for L = N-heterocyclic ligands.[39] This correlation is valuable since E_L is available in the literature and was proved to be useful in previously estimating the *trans*-$[Ru(NH_3)_4L(NO)]^{3+/2+}$ redox potential.

It is important to stress that, depending on the electronic characteristics of L, the latter could be displaced instead of NO. In complexes where Cl^- is localized trans to NO,[24,25] as in *trans*-$[Ru(NH_3)_4(Cl)(NO)]^+$, *trans*-[Ru(cyclam)-$(Cl)(NO)]^+$ and *trans*-[Ru(dppe)$(Cl)(NO)]^+$, chloride is preferentially released before NO.

In contrast to the inertia of the $Ru^{II}NO^+$ species, the lability of NO in $Ru^{II}NO^0$ species seems to be common in species where L is a π-acid and should reflect the strength of the Ru−NO bond in both species. To investigate the origin of this different behavior, DFT computations for *trans*-$[Ru(NH_3)_4(L)(NO)]^{3+}$ and *trans*-$[Ru(NH_3)_4(L)(NO)]^{2+}$ (L = py) were performed. The results obtained in terms of bond lengths and bond angles are similar to those reported for the two systems:[40] $[Ru(CN)_5(NO)]^{2-}$ and $[Ru(CN)_5(NO)]^{3-}$,[41] $[Ru(NH_3)_5(NO)]^{3+}$ and $[Ru(NH_3)_5$-$(NO)]^{2+}$ (Table 2).

The MO composition (see Table 3) for *trans*-$[Ru(NH_3)_4(L)(NO)]^{3+}$ shows that the π interaction between Ru^{II} and NO^+ consists of a combination of the filled d_{xy} and d_{xz} orbitals (Ru) and the double degenerate, empty π* orbitals of nitric oxide besides the p_y* orbitals of pyridine: HOMO-5 (Ru d_{xy} 33 %, NO p_y 11 %, py p_y 54 %) and HOMO-6 (Ru d_{xz} 69 %, NO p_z 22 %, py p_z 6 %). Figure 4 (left) shows the HOMO-6 graphical representation of *trans*-$[Ru(NH_3)_4(py)(NO)]^{3+}$. The percentage [11−22 % (π* NO)] in the HOMO-5 and HOMO-6 orbitals is consistent with the well-known back bonding from Ru^{II} to NO^+, while 54 % for py (p_y) in the HOMO-5 orbital, which could be considered responsible for the influence of the *trans* ligand on the NO electronic density, is reflected on the $[Ru^{II}NO^+/Ru^{II}NO^0]$ redox potential and ν_{NO}, as observed.

As expected, the LUMO and LUMO+1 for the *trans*-$[Ru(NH_3)_4(L)(NO)]^{3+}$ complexes [an example of these molecular orbitals is shown in Figure 4 (right)] are antibonding with relation to the Ru−NO π-bond. These π-antibonding orbitals are predominantly on NO π* (66−69 %) (Table 3), which is in agreement with the formation of *trans*-$[Ru(NH_3)_4(L)(NO)]^{2+}$ as a result of *trans*-$[Ru(NH_3)_4(L)(NO)]^{3+}$ one-electron reduction and with the additional electron occupying one of these π* MOs. Indeed, a similar DFT MO calculation performed on *trans*-$[Ru(NH_3)_4(L)(NO)]^{2+}$ agrees with this prediction and the singly occupied MO (HOMO) and the LUMO, which correspond to the LUMO and LUMO+1 of *trans*-$[Ru(NH_3)_4(L)(NO)]^{3+}$, respectively, are composed of HOMO Ru (d_{xz}) 35 %, NO (p_z) 50 % and py (p_z) 13 % and LUMO Ru (d_{xy}) 28 %, NO (p_y) 70 % and py (p_y) 2 %. As expected from previous DFT calculations for the $[Ru(CN)_5(NO)]^{3-}$ and $[Ru(NH_3)_5(NO)]^{2+}$ systems,[40,41] a pronounced bend of 139° in the Ru−N−O angle is observed (Table 2). Although, a π-bonding interaction between Ru and NO still exists, that is, HOMO-3 and HOMO-4 [see Table 4 and an orbital representation in Figure 5 (left)], this Ru−*N*−O bending induces a considerable

Table 2. Selected theoretical bond lengths and angles calculated by DFT for (nitrosyl)ruthenium complexes

Complex	Ru−NO (Å)	N−O (Å)	Ru−*N*−O (deg)	Ref.
trans-$[Ru(NH_3)_4(py)(NO)]^{3+}$	1.820	1.130	180.0	this work
trans-$[Ru(NH_3)_4(py)(NO)]^{2+}$	1.910	1.174	139.0	this work
trans-$[Ru(NH_3)_4(nic)(NO)]^{3+}$	1.775	1.137	179.4	[42]
trans-$[Ru(NH_3)_5(NO)]^{3+}$	1.808	1.153	172.8	[40]
trans-$[Ru(NH_3)_5(NO)]^{2+}$	1.894	1.216	137.1	[40]
$[Ru(CN)_5(NO)]^{3+}$	1.770	1.176	180.0	[41]
$[Ru(CN)_5(NO)]^{2+}$	1.893	1.221	144.9	[41]

Table 3. Selected MO contribution in percentage for *trans*-$[Ru(NH_3)_4(py)(NO)]^{3+}$

			trans-$[Ru(NH_3)_4(py)(NO)]^{3+}$			
	eV	symm	Ru	NO	NH_3	L
LUMO	−15.2	π*	23 (d_{xy})	66 (p_y)	3	8 (p_y)
HOMO	−15.2	π*	26 (d_{xz})	69 (p_z)	4	1
HOMO-1	−18.3	nonbonding	0	0	4	96 (p_z)
HOMO-2	−18.8	nonbonding	4 (d_{xz})	5 (p_z)	4	87 (p_z)
HOMO-3	−19.7	nonbonding	68 (d_{z^2},$d_{x^2-y^2}$)	1	4	25 (s)
HOMO-4	−20.2	π*L	23 ($d_{x^2-y^2}$)	5 (s)	1	71 (p_x)
HOMO-5	−20.5	π	33 (d_{xy})	11 (p_y)	3	54 (s,p_x,p_y)
HOMO-6	−20.6	π	69 (d_{xz})	22 (p_z)	4	6 (p_z)

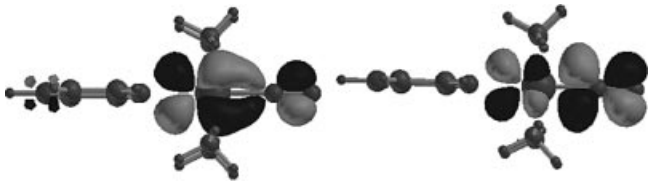

Figure 4. Molecular orbital description of a (nitrosyl)metal complex; (left) HOMO-6: ligand π interaction between Ru (either d_{xy} and d_{xz}) and NO π* orbitals (p_y* and p_z*); (right) LUMO: antiligand π interaction between Ru (either d_{xy} and d_{xz}) and the NO π* orbitals (p_y* and p_z*)

reduction of Ru and NO π-bonding [compare Figure 4 (left) and 5 (left)].

As a consequence, Ru−NO bond weakening is expected and it is comprehensible that the nitric oxide ligand is much more susceptible to dissociation in the *trans*-$[Ru(NH_3)_4(L)(NO)]^{2+}$ species than in the the oxidized analogues. Although, the HOMO and the LUMO for *trans*-$[Ru(NH_3)_4(L)(NO)]^{2+}$ ions, which were totally antibonding

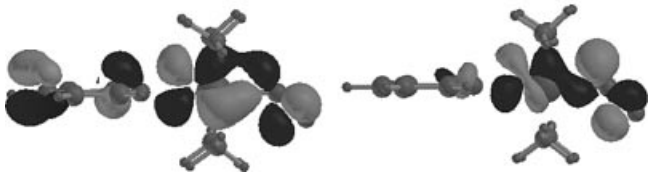

Figure 5. Molecular orbital interaction in a bent (nitrosyl)metal complex; (left) HOMO-3: bending the NO ligand minimizes the overlap between the metal orbitals (either d_{xy} and d_{xz}) and the NO π* orbitals (either p_y* and p_z*); (right) HOMO: the antibonding character presents a compensatory bonding interaction between the NO (p_z*) and the metal (d_{xz}) orbitals as Ru−*N*−O bend

MOs for *trans*-$[Ru(NH_3)_4(L)(NO)]^{3+}$ (LUMO and LUMO+1, respectively), assume a partial bonding character, they do not seem to be strong enough to keep the metal-coordination sphere intact, as observed. The calculated Ru−NO bond lengths for *trans*-$[Ru(NH_3)_4(L)(NO)]^{3+}$ (1.82 Å) and *trans*-$[Ru(NH_3)_4(L)(NO)]^{2+}$ (1.91 Å) are in agreement with the Ru−NO bond weakening (Table 2) and they are accompanied by a measurable lengthening of the N−O bond, from 1.130 Å to 1.174 Å (Table 2), which is consistent since the HOMO for the *trans*-$[Ru(NH_3)_4(py)(NO)]^{2+}$ ion has a considerable population and its composition is predominant on NO π* orbitals. As shown in Table 2, Ru−NO and N−O bond lengthening is usual as the same is also observed for $[Ru(CN)_5(NO)]^{3-}$ and $[Ru(NH_3)_5(NO)]^{2+}$ systems.[40,41]

Conclusion

The *trans*-$[Ru(NH_3)_4L(NO)]^{3+}$ complex ions are better described as formally $Ru^{II}NO^+$ and they are stable towards substitution reactions. Following activation by one-electron reduction, species having a labile NO^0 ligand are produced, which makes these compounds good NO-donor drug prototypes.

The rate of NO dissociation from the *trans*-$[Ru(NH_3)_4(L)(NO)]^{2+}$ and the *trans*-$[Ru(NH_3)_4L(NO)]^{3+/2+}$ redox potential, could be modulated by a judicious choice of the ligand, L. These two critical steps for NO-donor-drug designing can be predicted by plots of k_{-NO} versus ΣE_L and from the *trans*-$[Ru(NH_3)_4L(NO)]^{3+/2+}$ redox potential versus ΣE_L, respectively.

Table 4. Selected MO contribution in percentage for *trans*-$[Ru(NH_3)_4(py)(NO)]^{2+}$

			trans-$[Ru(NH_3)_4(py)(NO)]^{+2}$			
	eV	symm	Ru	NO	NH_3	L
LUMO	−9.7	π*	28 (d_{xy})	70 (p_y)	0	2 (p_y)
HOMO	−12.9	π*	35 (d_{xz})	50 (p_z)	2	13 (p_y)
HOMO-1	−14.1	nonbonding	87 (d_{z^2}; $d_{x^2-y^2}$)	0	5	8
HOMO-2	−14.5	nonbonding	0	0	3	97 (p_z,p_y)
HOMO-3	−14.5	π	44 (d_{xz})	26 (p_z)	2	28 (p_z)
HOMO-4	−14.5	π	58 (d_{xy})	20 (p_y)	3	19 (p_y,p_x)
HOMO-5	−15.3	π*L	24 (d_{xz})	6 (p_z)	2	68 (p_z)

Experimental Section

Chemicals and Reagents: High purity chemicals (Aldrich) were used as supplied. $RuCl_3$ was obtained from Johnson Matthey. All solvents were purified following the known procedures.[43] Doubly distilled water was used throughout the experiments. All preparations and measurements were performed under argon. $[Ru(NH_3)_5Cl]Cl_2$,[44] *trans*-$[Ru(NH_3)_4(SO_2)(Cl)]Cl$,[45,46] *trans*-$[Ru(NH_3)_4(SO_4)(L)]Cl$[47] and *trans*-$[Ru(NH_3)_4(L)(NO)](BF_4)_3$[21,22] were prepared as described previously. ESR spectra were recorded in a Bruker ESP 300 E spectrophotometer at the temperature of liquid nitrogen. Electrochemical measurements were performed in both an EG&G Princeton Applied Research model 264A Par and an Autolab potentiostat/galvanostat PGSTAT30. Experiments were conducted using a glassy carbon or gold disks as working electrodes, a saturated calomel electrode (SCE) as a reference electrode and a platinum wire as an auxiliary electrode. The supporting electrolyte consisted of an aqueous buffer solution (pH = 5.0 at μ = 0.1 maintained with $NaCH_3COO/CH_3COOH$) kept under argon atmosphere during measurements. Electrolysis experiments were performed on an EG&G PARC model 173/interface model 276 potentiostat/galvanostat using an optically transparent gold minigrid as a working electrode, Ag/AgCl as a reference electrode and a platinum wire as auxiliary electrode, in a 0.1 cm quartz cell. Spectral changes during the electrolysis were recorded in an HP 8453 diode-array spectrophotometer.

Infrared spectra in aqueous solution (pH = 4) were performed in a calcium fluoride cell in an FTIR Bomen MB-102 spectrometer.

Kinetic experiments were conducted by double-potential-step chronoamperometry. The potential was briefly stepped from a value in which the compound is not reduced at the electrode surface to one in which the reduction proceeds at diffusion-controlled rate. After a period of time, the potential was stepped back to a potential in which the reduced form is oxidized. The kinetic information is obtained from the ratio between the currents measured on both potential steps as a function of time and by comparing these data with those obtained from working curves described in the literature.[48]

All the calculations were performed using the Gaussian 98 suite of programs.[49] The starting molecular geometries were obtained at the UHF/3−21G level of theory.[50−52] The final molecular geometry optimizations were performed using the Kohn−Shan density functional theory (DFT)[53−56] with the 6−31(d) basis set for the H, C, N, O, and P atoms, and an effective core potential LanL2DZ[57−59] for the Ru atom and the Becke three-parameters hybrid exchange-correlation functional known as B3LYP.[60−62] The analytical evaluation of the derivative matrix cartesian coordinates of the second energy (Hessian matrix) at the same level of approximation confirmed the nature of the minimum of the potential surface points associated to the optimized structures.

Acknowledgments

The authors would like to acknowledge Bruce R. McGarvey for reading the manuscript and the Brazilian foundations FAPESP (processes numbers 1999/07109−9, 99/11252−1 and 01/08563−7), CNPq and Capes for their financial support and also Johnson Matthey for supplying the $RuCl_3$ compound.

[1] L. J. Ignarro, *Pharmacol. Res.* **1989**, *6*, 651−659.
[2] S. Moncada, R. M. J. Palmer, E. A. Higgs, *Pharm. Rev.* **1991**, *43*, 109−142.
[3] M. J. Clarke, *Coord. Chem. Rev.* **2003**, *236*, 209−233.
[4] P. G. Wang, M. Xian, X. P. Tang, X. J. Wu, Z. Wen, T. W. Cai, A. J. Janczuk, *Chem. Rev.* **2002**, *102*, 1091−1134.
[5] F. Bottomley, *Reaction of Coordinated Ligands* (Ed: P. S. Braterman) Plenum Press, New York **1992**, chapter 3.
[6] G. B. Richter-Addo, P. Legzdins, *Metal Nitrosyls*, New York Ed, New York, **1992**, 271−333.
[7] T. W. Hayton, P. Legzdins, W. B. Sharp, *Chem. Rev.* **2002**, *102*, 935−991.
[8] C. S. Allardyce, P. J. Dyson, *Platinum Met. Rev.* **2001**, *45*, 62−69.
[9] E. Tfouni, M. H. Krieger, B. R. McGarvey, D. W. Franco, *Coord. Chem. Rev.* **2002**, *236*, 57−69.
[10] S. P. Fricker, *Platinum Met. Rev.* **1995**, *39*, 150−159.
[11] S. P. Fricker, E. Slade, N. A. Powell, O. J. Vaughan, G. R. Henderson, B. A. Murrer, I. L. Megson, S. K. Bisland, F. W. Flitney, *Br. J. Pharmacol.* **1997**, *122*, 1441−1449.
[12] Y. Chen, R. E. Shepherd, *J. Inorg. Biochem.* **1997**, *68*, 183−193.
[13] B. R. Cameron, M. C. Darkes, H. Yee, M. Olsen, S. P. Fricker, R. T. Skerlj, G. J. Bridger, N. A. Davies, M. T. Wilson, D. J. Rose, J. Zubieta, *Inorg. Chem.* **2003**, *42*, 1868−1876.
[14] B. R. Cameron, M. C. Darkes, I. R. Baird, R. T. Skerlj, Z. L. Santicci, S. P. Fricker, *Inorg. Chem.* **2003**, *42*, 4102−4108.
[15] B. F. Barros, J. C. Toledo Jr., D. W. Franco, E. Tfouni, M. H. Krieger, *Biochem., Pharmacol. Clin. Aspects Nitric Oxide* **2002**, *7*, 50−56.
[16] A. S. Torsoni, B. F. Barros, J. C. Toledo Jr., M. Hawn, M. H. Krieger, E. Tfouni, D. W. Franco, *Biochem., Pharmacol. Clin. Aspects Nitric Oxide* **2002**, *6*, 247−254.
[17] O. Siri, A. Tabard, P. Pullumbi, R. Guilard, *Inorg. Chim. Acta* **2003**, *350*, 633−640.
[18] P. C. Ford, J. Bourassa, K. Miranda, B. Lee, I. Lorkovic, S. Boggs, S. Kudo, L. Laverman, *Coord. Chem. Rev.* **1998**, *171*, 185−202.
[19] P. C. Ford, I. M. Lorkovic, *Chem. Rev.* **2002**, *102*, 993−1017.
[20] L. G. F. Lopes, A. Wieraszko, Y. EL-Sherif, M. J. Clarke, *Inorg. Chim. Acta* **2001**, *312*, 15−22.
[21] S. S. S. Borges, C. U. Davanzo, E. E. Castellano, J. Z-Schpector, S. C. Silva, D. W. Franco, *Inorg. Chem.* **1998**, *37*, 2670−2677.
[22] M. G. Gomes, C. U. Davanzo, S. C. Silva, L. G. F. Lopes, R. H. A. Santos, D. W. Franco, *J. Chem. Soc., Dalton Trans.* **1998**, *37*, 601−607.
[23] P. C. Ford, *Coord. Chem. Rev.* **1970**, *5*, 75−89.
[24] C. W. B. Bezerra, S. C. Silva, M. T. P. Gambardella, R. H. A. Santos, L. M. A. Plicas, E. Tfouni, D. W. Franco, *Inorg. Chem.* **1999**, *38*, 5660−5667.
[25] L. G. F. Lopes, E. E. Castellano, J. Z-Schpector, A. G. Ferreira, C. U. Davanzo, M. J. Clarke, D. W. Franco, *in preparation*.
[26] F. Roncaroli, M. E. Ruggiero, D. W. Franco, G. L. Estiú, J. A. Olabe, *Inorg. Chem.* **2002**, *41*, 5760 −5769.
[27] S. I. Gorelsky, S. C. Silva, A. B. P. Lever, D. W. Franco, *Inorg. Chim. Acta* **2000**, *300*, 698−708.
[28] B. R. McGarvey, A. A. Ferro, E. Tfouni, C. W. B. Bezerra, I. Bagatin, D. W. Franco, *Inorg. Chem.* **2000**, *39*, 3577−3581.
[29] R. W. Callahan, T. J. Meyer, *Inorg. Chem.* **1977**, *16*, 574−581.
[30] Y. Chen, F. T. Lin, R. E. Shepherd, *Inorg. Chem.* **1999**, *38*, 973−983.
[31] V. Mori, J. C. Toledo Jr., H. A. S. Silva, D. W. Franco, M. Bertotti, *J. Electroanal. Chem.* **2003**, *547*, 9−15.
[32] H. A. S. Silva, B. R. McGarvey, R. H. A. Santos, M. Bertotti, V. Mori, D. W. Franco, *Can. J. Chem.* **2001**, *79*, 679−687.
[33] D. R. Lang, J. A. Davis, L. G. F. Lopes, A. A. Ferro, L. C. G. Vasconcellos, D. W. Franco, E. Tfouni, A. Wieraszko, M. J. Clarke, *Inorg. Chem.* **2000**, *39*, 2294−2300.
[34] S. S. Isied, H. Taube, *Inorg. Chem.* **1976**, *15*, 3070−3075.
[35] D. W. Franco, *Coord. Chem. Rev.* **1992**, *119*, 199−225.
[36] A. B. P. Lever, *Inorg. Chem.* **1990**, *29*, 1271−1285.
[37] L. Stryer, *Biochemistry 2nd Ed.,* W. H. Freeman and Company: New York, **1981**,235−254.

[38] J. C. Toledo Jr., L. G. F. Gonzaga, A. A. Alves, L. P. Silva, D. W. Franco, *J. Inorg. Biochem.* **2002**, *89*, 267−271.
[39] L. G. F. Lopes, M. G. Gomes, S. S. S. Borges, D. W. Franco, *Aust. J. Chem.* **1998**, *51*, 865−866.
[40] M. Wanner, T. Scheiring, W. Kaim, L. D. Slep, L. M. Baraldo, J. A. Olabe, E. J. Baerends, *Inorg. Chem.* **2001**, *40*, 5704−5707.
[41] J. C. Patterson, I. M. Lorkovic, P. C. Ford, *Inorg. Chem.* **2003**, *42*, 4902−4908.
[42] C. Kim, I. Novozhilova, M. S. Goodman, K. A. Bagley, P. Coppens, *Inorg. Chem.* **2000**, *39*, 5791−5795.
[43] D. D. Perrin, W. L. F. Armarego, D. P. Perrin, *Purification of Laboratory Chemicals*, 3 rd ed, Pergamon Press: New York, **1983**, 65−310.
[44] A. D. Allen, F. Bottomley, R. D. Harris, V. P. Reinslau, C. V. Senoff, *Inorg. Synth.* **1970**, *12*, 2−11.
[45] K. Gleu, W. Breuel, K. Z. Rehm, *Z. Anorg. Allg. Chem.* **1938**, *235*, 201−208.
[46] L. H. Vogt, J. L. Katz, S. E. Wiberley, *Inorg. Chem.* **1965**, *4*, 1157−1163.
[47] G. M. Brown, J. E. Sutton, H. Taube, *J. Am. Chem. Soc.* **1978**, *100*, 2767−2774.
[48] A. J. Bard, L. A. Faulkner, *Electrochemical Methods: Fundamentals and Applications*, John Wiley & Sons, New York, **1980**, 176−183.
[49] M. J. Frisch, G. W. Trucks, H. B. Schlegel, G. E. Scuseria, M. A. Robb, J. R. Cheeseman, V. G. Zakrzewski, J. A. Montgomery, Jr., R. E. Stratmann, J. C. Burant, S. Dapprich, J. M. Millam, A. D. Daniels, K. N. Kudin, M. C. Strain, O. Farkas, J. Tomasi, V. Barone, M. Cossi, R. Cammi, B. Mennucci, C. Pomelli, C. Adamo, S. Cli. ord, J. Ochterski, G. A. Petersson, P. Y. Ayala, Q. Cui, K. Morokuma, D. K. Malick, A. D. Rabuck, K. Raghavachari, J. B. Foresman, J. Cioslowski, J. V. Ortiz, B. B. Stefanov, G. Liu, A. Liashenko, P. Piskorz, I. Komaromi, R. Gomperts, R. L. Martin, D. J. Fox, T. Keith, M. A. Al-Laham, C. Y. Peng, A. Nanayakkara, C. Gonzalez, M. Challacombe, P. M. W. Gill, B. Johnson, W. Chen, M. W. Wong, J. L. Andres, C. Gonzalez, M. Head-Gordon, E. S. Replogle, J. A. Pople, *Gaussian 98*, Revision A.6, Gaussian, Inc., Pittsburgh, PA (**1998**).
[50] C. C. J. Roothan, *Rev. Mod. Phys.* **1951**, *23*, 69−75.
[51] J. A. Pople, R. K. Nesbet, *J. Chem. Phys.* **1954**, *22*, 571−572.
[52] R. McWeeny, G. Dierksen, *J. Chem. Phys.* **1968**, *49*, 4852−4856.
[53] P. Hohenberg, W. Kohn, *Phys. Rev. Sect. B* **1964**, *136*, 864−871.
[54] W. Kohn, L. J. Sham, *Phys. Rev. Sect. A* **1965**, *140*, 1133−1138.
[55] A. D. Becke, *J. Chem. Phys.* **1993**, *98*, 5648−5652.
[56] R. G. Parr, W. Yang, *Density-Functional Theory of Atoms and Molecules*, Oxford Univ. Press, Oxford, **1989**, 142−197.
[57] P. J. Hay, W. R. Wadt, *J. Chem. Phys.* **1985**, *82*, 270−283.
[58] W. R. Wadt, P. J. Hay, *J. Chem. Phys.* **1985**, *82*, 284−298.
[59] P. J. Hay, W. R. Wadt, *J. Chem. Phys.* **1985**, *82*, 299−310.
[60] A. D. Becke, *J. Chem. Phys.* **1993**, *98*, 5648−5652.
[61] C. Lee, W. Yang, R. G. Parr, *Phys. Rev. Sect. B* **1988**, *37*, 785−789.
[62] A. D. Becke, *Phys. Rev. A* **1988**, *38*, 3098−3100.

Received September 29, 2003
Early View Article
Published Online March 23, 2004

